
HIERARCHICAL NEURAL ARCHITECTURE SEARCH VIA OPERATOR CLUSTERING

Li Guilin¹, Zhang Xing¹, Jiashi Feng², Wang Zitong¹, Matthias Tan⁴, Li Zhenguo¹, Zhang Tong⁵
¹Huawei Noah’s Ark Lab, ¹NUS, ⁴CityU, ⁵HKUST
{ hiliguilin@gmail.com, zhang.xing1@huawei.com, tongzhang@tongzhang-ml.org }

ABSTRACT

Recently, the efficiency of automatic neural architecture design has been significantly improved by gradient-based search methods such as DARTS. However, recent literature has brought doubt to the generalization ability of DARTS, arguing that DARTS performs poorly when the search space is changed, i.e. when different set of candidate operators are used. Regularization techniques such as early stopping have been proposed to partially solve this problem. In this paper, we tackle this problem from a different perspective by identifying two contributing factors to the collapse of DARTS when the search space changes: (1) the correlation of similar operators incurs unfavorable competition among them and makes their relative importance score unreliable and (2) the optimization complexity gap between the proxy search stage and the final training. Based on these findings, we propose a new hierarchical search algorithm. With its operator clustering and optimization complexity match, the algorithm can consistently find high-performance architecture across various search spaces. For all the five variants of the popular cell-based search spaces, the proposed algorithm always obtains state-of-the-art architecture with best accuracy on the CIFAR-10, CIFAR-100 and ImageNet over other well-established DARTS-alike algorithms. Code is available at <https://github.com/susan0199/StacNAS>.

1 Introduction

Recent years have witnessed the rapid development of automatic neural architecture design since introduction of NAS by Zoph et al [1]. To further improve search efficiency, recent work has explored various one-shot architecture search methods [2, 3, 4, 5, 6, 7], by using supernet and weight sharing to reduce the cost of training. Among those models, DARTS [3] relaxes the discrete search space to be continuous so that stochastic gradient descent can be applied to simultaneously learn the architectures and model parameters.

However, some recent works have demonstrated one important search collapse problem of DARTS, i.e., the algorithm tends to converge to a cell with all skip-connections, giving under-performing architectures. To address this problem, Arber et.al [8] proposed several regularization techniques to find optima with better generalization property and reported improved results across several variants of DARTS search spaces. However, in our experiments, we found that these regularization techniques do not work well on every search space we experimented with, driving us to further improve their results on the generalization ability of DARTS from different perspectives. We identify two core issues that lead to the above failure of DARTS-alike algorithms, i.e., the correlation among operators in the supernet; and the optimization complexity gap between the proxy search stage and final training stage.

More concretely, the first factor is the *correlation of similar operators* such as *SepConv* 3×3 and *SepConv* 5×5 , as illustrated in Figure 1. To calculate this correlation matrix, we first flatten the output feature map tensor into vectors of each operator at a fixed node, and then calculate the Pearson correlation coefficient between any two of the candidate operators. When some operators producing highly correlated feature maps, their contribution to the network search should be considered jointly. Otherwise, the architecture parameter cannot be estimated accurately because their contribution score would be decreased due to such unfavorable within-group competition.

The second factor that affects the search performance dramatically is *the gap between the optimization complexity of the proxy search stage and the final training stage*. It is known that skip-connections are crucial to the training of deep CNN models even though they may not be so important for the shallower ones. In DARTS, the author first uses a shallow proxy network with eight-cells to search for the optimal cell structures, and then repeats the discovered cells to form a much deeper 20-cells final structure. This gap causes the search algorithm to select more than enough complicated operators such as convolution. We empirically find when the parent architecture in the proxy search space is too shallow, the algorithm would tend to select fewer skip connections; however when the parent architecture is too deep, the algorithm would select more than the optimal number of skip connections. By using **gradient confusion** [9] to measure and explain the optimization complexity gap problem, we show that a proper depth must be selected if a smaller supernet is used in the proxy search stage. This complexity matching is essential for the algorithm to select an appropriate number of skip-connections for the target networks with different depths, while the vanilla DARTS fails to do so.

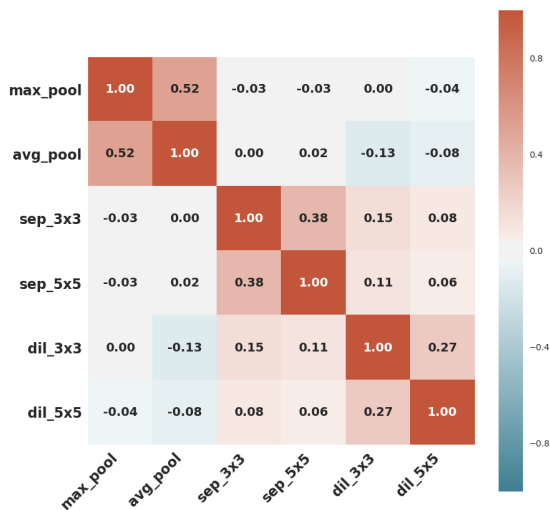


Figure 1: Operator correlation matrix: pairwise correlation between flattened feature map of candidate operators. The details of the correlation calculation procedure are provided in the Appendix A.

To solve these problems, we introduce a new hierarchical search algorithm that performs operator clustering and optimization complexity matching. In the first stage of the algorithm, the best group is activated, and in the second stage, the best operator in the activated group is selected. This hierarchical search algorithm would select proper operators with matching complexities more accurately, and yield a more STable and Consistent differentiable Neural Architecture Search method, we name this method as **StacNAS**.

By solving these two problem, our proposed algorithm can generalize well to different variants of the cell-based search space, where the other existing DARTS-alike algorithms yield degenerate or unstable results. In our experiments, we show that the proposed hierarchical search algorithm is able to find a convolutional cell that achieves a test error of 2.33% on CIFAR-10 and a top-1 error of 24.17% on IMAGENET for an image classification task. This is the current state-of-the-art result among all DARTS-alike methods based on the original cell-based search space and control of the final training hyper-parameters as in DARTS. We also conducted extensive experiments on four variants of DARTS search spaces and compare the generalization ability of five state-of-the-art DARTS-alike algorithm, including DARTS [3], CARS [7], PC-DARTS [10], and DARTS-ES [8] on CIFAR10. On all these four spaces, our method StacNAS performs the best.

2 Related Work

Due to its efficiency and effectiveness for the NAS task, DARTS has attracted a lot of attention. Cai et al. [6] propose ProxylessNAS using path sampling during the search to reduce the high memory cost of DARTS. Realizing the depth gap between the search stage (a shallow network of 8 cells is used) and the final architecture (the discovered cell is repeated to stack a 20 cells structure), Chen et al. [11] proposed PDARTS to progressively prune the search space and deepen the search network. In the analysis we present later, it is shown that this pruning of the search space is harmful. Specifically, it results in an imbalanced number of operators in different groups: i.e. more Convolution operators than Pooling. PDARTS tries to bridge the depth gap by manually tuning the depth used and controlling the number of skip connections to obtain better performance on CIAR10. In this work, we go one step further. We identify the root cause of the problem as the optimization complexity gap due to use of a shallow proxy structure to search for the cell structure for a deeper final structure. This causes the search stage to converge to a cell with an improper number of skip connections. Arber et al. [8] examine DARTS on several variants of the search spaces, and propose to robustify DARTS by using regularization tricks such as early stopping. In this work, we tackle the robustness problem of DARTS by analyzing two root causes of failure/instability of DARTS, i.e., the linear correlation of similar operators and the optimization complexity gap.

3 When and Why DARTS Fails

3.1 Preliminaries

We use the cell-based search space of DARTS, where a convolutional neural network is formed by stacking a series of building blocks called cells [12, 3]. Only two types of cells are learned: the *normal cell* and the *reduction cell*. A cell can be seen as a directed acyclic graph (DAG), where an ordered sequence of N nodes $\{x_1, \dots, x_N\}$ are connected by directed edges (i, j) . Each node x_i is a latent representation (i.e. a feature map) and each directed edge (i, j) represents some operator $o(\cdot) \in O$ that transforms x_i . Within a cell, each internal node is computed as the sum of all its predecessors: $x_j = \sum_{i < j} o^{(i,j)}(x_i)$. The task of designing the cell structure is to determine the most important two preceding edges for all internal nodes and the best choice of operators for these selected edges.

DARTS [3] proposed a continuous relaxation of the categorical choice of operators and edges so that their relative importance can be learned through stochastic gradient descent (SGD). Specifically, to make the search space continuous, DARTS replaces the discrete choice of operator $o(\cdot) \in O$ with a weighted sum over all candidate operators $\bar{o}^{(i,j)}(x) = \sum_{o \in O} \alpha_o^{(i,j)} o^{(i,j)}(x_i)$ where $\alpha_o^{(i,j)} = \frac{\exp(\beta_o^{(i,j)})}{\sum_{o' \in O} \exp(\beta_{o'}^{(i,j)})}$ is called the architecture parameters.

After the relaxation, the task of architecture search reduces to learning a set of continuous architecture parameters $\alpha = \{\alpha^{(i,j)}\}$. Specifically, one first trains a proxy supernet that contains all candidate operators and connections/edges. During training, one would be able to learn which operators and edges are redundant. After the training algorithm converges, a compact architecture is obtained by pruning the unimportant operators and edges.

In DARTS, [13] formulate the optimization of the architecture parameters α and the weights w associated with the architecture as a bi-level optimization problem, where α is treated as the upper-level variable and w as the lower-level variable:

$$\min_{\alpha} L_{val}(w^*(\alpha), \alpha), \quad \text{s.t. } w^*(\alpha) = \operatorname{argmin}_w L_{train}(w, \alpha), \quad (1)$$

where L_{train} and L_{val} denote the training and validation loss respectively.

3.2 Examining DARTS on Different Search Spaces

The Failure Pattern To examine the generalization problem of the DARTS-alike algorithms, we use the following five search spaces **S1** to **S5**. **S1** is the original DARTS search space where each type of operators has two members except for *SkipConnect*. For example, there are two pooling operators and two SepConv operators. To examine the correlation problem, in **S2**, we add more pooling to the search space and in **S3** we add more convolution to the search space. In **S4**, all poolings are removed and in **S5** we use a search space with the most frequent operators in the searched cells reported by [3] to mimic the progressive pruning process proposed in [11]:

- **S1**: {*MaxPooling* 3×3 , *AvePooling* 3×3 , *SepConv* 3×3 , *SepConv* 5×5 , *DilConv* 3×3 , *DilConv* 5×5 , *SkipConnect*, *Zero*}
- **S2**: {*MaxPooling* 3×3 , *MaxPooling* 5×5 , *AvePooling* 3×3 , *AvePooling* 5×5 , *SepConv* 3×3 , *SepConv* 5×5 , *SkipConnect*, *Zero*}
- **S3**: { *MaxPooling* 3×3 , *SepConv* 3×3 , *SepConv* 5×5 , *SepConv* 7×7 , *DilConv* 3×3 , *DilConv* 5×5 , *SkipConnect*, *Zero* }
- **S4**: {*SepConv* 3×3 , *SepConv* 5×5 , *DilConv* 3×3 , *DilConv* 5×5 , *SkipConnect*, *Zero*}
- **S5**: { *SepConv* 3×3 , *SkipConnect*, *Zero* }

Note that Zero operator here serves as a scaling of each edge, allowing the scoring of the contribution of each edge.

Table 1: Results of DARTS on various search space base on CIFAR10. Random Baseline is obtained by evaluating 4 randomly generated architectures from the search spaces.

Search Space	Random Baseline	DARTS Test Error	Characteristics (normal cell)
S1 original	96.90 ± 0.23	97.03 ± 0.32	Mixed
S2 more pooling	96.59 ± 0.60	96.78 ± 0.20	All operators are SepConv
S3 more convolution	97.14 ± 0.16	91.87 ± 3.30	All operators are SkipConnect
S4 no pooling	96.81 ± 0.15	88.36 ± 5.10	All operators are SkipConnect
S5 less convolution	97.31 ± 0.15	95.67 ± 1.20	All operators are SkipConnect

Table 2: Results of DARTS on CIFAR10 by using different supernet depth during search.

Supernet depth (No. of cells)	5	14	17	20
No.of SkipConnect in normal cell	0	2	3	4
Test Error	2.95 ± 0.23	2.75 ± 0.21	2.91 ± 0.27	3.14 ± 0.23

By examining DARTS on search space S1-S5, we found that DARTS performs poorer than the random baseline on three of them (see Table 1), which means, the search process is not only a waste of GPU time but also results in poorer architecture than a randomly generated one. By taking a closer look at the characteristics of the cells found by DARTS, we see that when the search space contains more pooling, DARTS tends to find a cell dominated with Convolution (Sep or Dil); when the search space contains more convolution, DARTS tends to end up with a cell dominated with Pooling or SkipConnection.

Why It Fails This phenomenon shows that when a certain group of operator (for example convolution operator) has more group members, the search algorithm would less likely choose it. We hypothesize that operators from the same group may serve similar functions/contributions to the final prediction, and hence they would compete for the final importance score assigned to this group. Indeed, the construction of the continuous search space as described in Section 3.1 is very similar to a multiple regression model: feature maps transformed by all candidate operators are summed together and weighted by coefficients α . Thus, when operators are producing highly correlated feature maps, their weights α may no longer be representative of their real importance. However, in DARTS, the relative importance of operator o is learned through the value of α_o .

For example, consider the search space S3. Suppose the system assigns SepConv a score of 0.6 and MaxPool a score of 0.3. However, there are three SepConvs in the system serving a similar function, so they would compete with each other and each gets a score of 0.2. Based on the rule of DARTS, MaxPool has a higher importance score of 0.3, so the system would choose MaxPool for this edge.

To verify this conjecture, we calculate the correlation between the flattened feature map of two operators for the first edge of the first cell in the converged supernet of DARTS. The results presented in Figure 1 shows that the total operators cluster to four groups (see Figure 2).

3.3 The Effect of Supernet Depth and Optimization Complexity Gap

The Failure Pattern In the supernet of DARTS, all the candidate operators have to be updated at each gradient step, which incurs large memory cost. A typical solution adopted by a DARTS-alike algorithm [3, 8, 10] is to shrink the width and the depth of the proxy supernet during the search stage. For example, in DARTS, during the search stage, a proxy supernet with a 16-channel width and an 8-cell depth is used. After the search converges and redundant operators and edges are pruned, the discovered cell is enlarged and repeated to obtain a 36-channel and 20-cell final structure. We examine the performance of DARTS using different numbers of stacked cells for the search stage, and found that the search results are very sensitive to this depth. As shown in Table 2, when the search stage architecture in the proxy search space is too shallow, the algorithms would tend to select fewer skip connections and when the search stage architecture is too deep, the algorithm would select more than the optimal number of skip connections. For example, when we increase the number of cells used for the search stage from 5 to 20, the number of skip connections in the normal cell will increase from 0 to 4.

Why It Fails We argue that the unstable result of DARTS when using different cells for the search stage than the final structure is due to **the optimization complexity gap between the proxy search stage and the final architecture**. As is well studied [14, 9], including skip connections would make the gradient flows easier and optimization of the deep neural network more stable. In DARTS, to save memory, a shallow network with 8 cells are used for the search stage and a deep network with 20 cells are used for the final architecture. This depth gap causes a huge optimization complexity gap between them, and the system would not be able to foresee the optimization difficulty when the cells are stacked to a much deeper network. An improper number of skip-connections may be selected as a result.

3.4 Hierarchical Search via operator Clustering

3.4.1 Two-stage Search via Operator Clustering

To remedy this problem, we propose a two-stage hierarchical search strategy through operator clustering. The correlation matrix presented in Figure 1 suggests that *MaxPool* and *AvePool* are in one group (their correlation

is 0.52), 3×3 and 5×5 *SepConv* are in the same group (correlation 0.38), 3×3 and 5×5 *DilConv* are in the same group (correlation 0.27). Therefore, we group all the operators to four clusters as shown in Figure 2.

In the first stage of the algorithm, the best group (for example, *SepConv*) is activated; and in the second stage, the best operator in the activated group is selected (for example *SepConv* 3×3) as shown in Figure 3.

3.4.2 Optimization Complexity Matching

As studied in [9], the key factors that affect the optimization difficulty include the width, the depth and the number of SkipConnect. Narrowing the network, deepening the network, and including fewer SkipConnect increase the optimization difficulty. In DARTS, both the width and the depth are changed for the proxy search supernet. Therefore, to select a proper number of SkipConnect, one must shrink the network in a balanced way.

To quantify the optimization difficulty more concretely, we use a criterion called gradient confusion, introduced in [9]. The authors empirically show that when gradient confusion is low, SGD has better convergence properties. Deeper networks usually correspond to higher gradient confusion, and skip connection can significantly reduce gradient confusion.

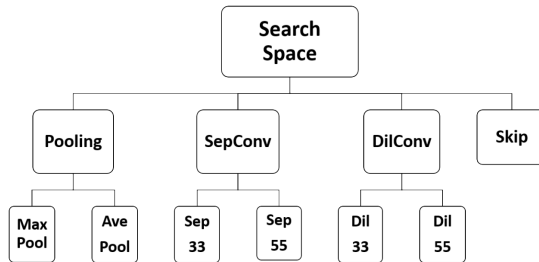


Figure 2: Operator clustering diagram: the search space clusters to four groups.

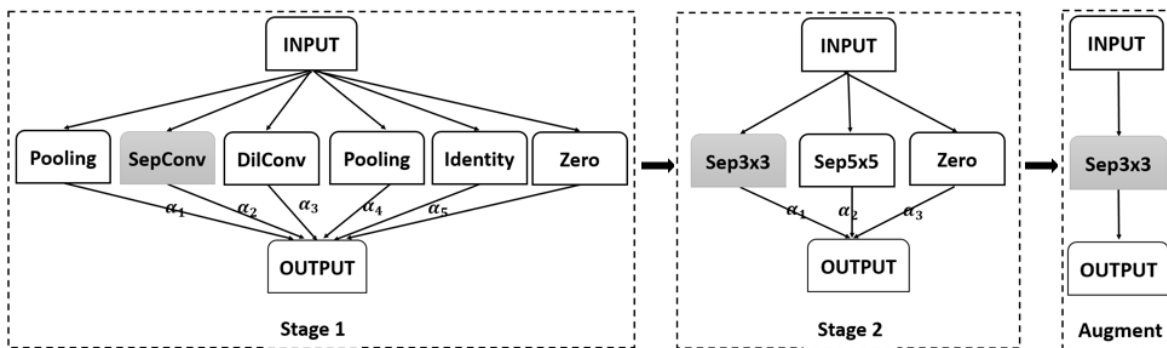


Figure 3: An overview of the algorithm: (a) Improved DARTS by placing a by-group mixture of candidate operators on each edge. (b) When a certain type of operator is activated, include all candidate operators in this type to form a new mixture operator. (c) Derive the final architecture.

Formally, let $\{l_i\}_{i=1}^m$ be losses for mini-batches, and let w be trainable parameters. *Gradient confusion* is defined to be the maximum value of the negative inner product between gradients evaluated at all mini-batches which is defined by the following formula:

$$\zeta = \max_{i,j=1,\dots,m} \{-\langle \nabla l_i(w), \nabla l_j(w) \rangle\}.$$

In Table 6, we present the normalized estimated gradient confusion (ζ is divided by the number of parameters) for both search stage and final architecture with different depth and a fixed width of 16 channels (estimation details are provided in the Appendix C). We can see that the desired depth for search stage 1 is 14 cells, to make the optimization complexity compatible with that of the final architecture. This matching enables the proposed algorithm to optimize the search architecture with the same level of difficulty as with the final architecture.

Empirically, we found that the search results are sensitive to the depth/width design of search stage 1 but are insensitive to the depth/width design of search stage 2. This seems to be due to the fact the number of skip connections are already determined in search stage 1. To facilitate easy use of the algorithm for different memory constraints, we provide several settings with different depth/width in Table 6 of Section 4.

3.4.3 One-level Optimization

Recent works [15, 16] have shown that one-level optimization performs equally good or even better than the original two-level optimization proposed by DARTS [3]. In our ablation study in Section 4.3, we also verified that coupled with the proposed solution, one-level optimization is superior to two-level optimization with respect to both accuracy and stability. Therefore, in this work, we adopt the simpler one-level optimization approach, where the parameters are updated simultaneously using: $w_t = w_{t-1} - \eta_t \partial_w L_{train}(w_{t-1}, \alpha_{t-1})$ and $\alpha_t = \alpha_{t-1} - \delta_t \partial_\alpha L_{train}(w_{t-1}, \alpha_{t-1})$, where η_t and δ_t are learning rates.

4 Experiments

In this section, we validate the effectiveness of our proposed method for the image classification task.

4.1 NAS Benchmarks on CIFAR10/CIFAR100

Implementation Details We conduct our first set of experiments on CIFAR-10 and CIFAR-100 [17], each containing 50,000 training images and 10,000 test images. CIFAR-10 has 10 classes and CIFAR-100 has 100. For search space **S1-S5** (see Section 3.2), we first estimate the correlation matrix of all the candidate operators to identify the underlying groups for the given data (the estimation method and clustering results of **S1-S5** is provided in the Appendix Section A). Then we select the representative operators—for fair competition among groups, we prefer to select those with the same kernel size, i.e. 3×3 —for each group to obtain the search space of search stage 1. In our ablation study in Section 4.3, we show that the final results are not sensitive to the selection of the representative operators.

In the first stage, the proxy parent network of 14 cells is trained using one-level optimization for 80 epochs. After convergence, the optimal operator group is activated based on the learned α . In the second stage, we replace the mixed operator with a weighted sum of all operators in the activated group from stage 1. Then a proxy parent network by stacking 20 cells is trained using one-level optimization for 80 epochs.

When the best cells are identified by the search stage, they are stacked to build the final architecture. We evaluate the final architecture using exactly the same training scheme like DARTS for a fair comparison. More details are provided in the Appendix B.

Search Results The search results on the original DARTS search space (**S1**) are provided in Table 3 for CIFAR10 and Table 4 for CIFAR100.

We also conducted extensive experiments on search spaces **S2-S5** and compare StacNAS with five other well-established DARTS-alike algorithm, including DARTS [3], CARS [7], PC-DARTS [10], and Robust_DARTS [8] on CIFAR10. As we can see from the results plotted in Figure 4 (Table is provided in APPENDIX F), our algorithm performs the best across all the search spaces. .

Figure 4: Comparison of five search methods and random sampled architecture (4 seeds) from their respective search spaces. Methods above the diagonal outperform the random sampled ones, vice versa. Left: CIFAR10 benchmark across search space S2-S5; Right: Some results of DARTS excluded for better demonstration.

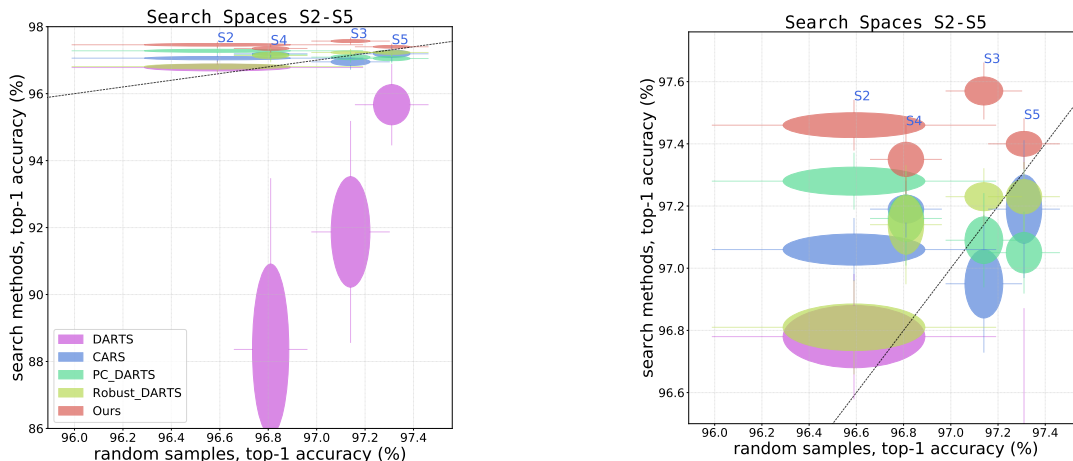


Table 3: CIFAR-10 Benchmark based on cell-based search space. * Proxyless reproduced by us on the cell-based search space.

Method	Test Error (%)	Optim
ENAS[18]	2.89	RL
CARS [7]	2.62	Evolution
DARTS [3]	2.76±0.09	Gradient
Proxyless[6]*	2.8 ± 0.2	Gradient
PDARTS [11]	2.5	Gradient
PC-DARTS [10]	2.57 ± 0.07	Gradient
Robust_DARTS [8]	2.95 ± 0.21	Gradient
StacNAS	2.48±0.08	Gradient

Table 4: CIFAR-100 Benchmark: * performed by us.

Method	Test Error (%)
DARTS*(base) [3]	17.63 ± 0.67
PDARTS (base) [11]	15.92
Robust_DARTS [8]	18.01 ± 0.26
StacNAS	15.41±0.2

Table 5: ImageNet Benchmark (mobile setting). IMAGENET(base) represents that the architecture are trained the same as DARTS. (AA) represents that the architecture are trained with AutoAugmentation.

Architecture	Test Error (%)		Params (M)	GPU Days	Search Method	Search Space
	top-1	top-5				
AmoebaNet-C [19]	24.3	7.6	6.4	3150	evolution	Cell-based
DARTS [3]	26.7	8.7	4.7	N/A	SGD	Cell-based
PDARTS [11]	24.4	7.4	4.9	N/A	SGD	Cell-based
PC-DARTS [10]	24.2	7.3	5.3	3.8	SGD	Cell-based
EfficientNet-B0 [20]	23.7	6.8	5.3	N/A	RL	MobileNet Backbone
StacNAS (base)	24.17	6.9	5.7	20	SGD	Cell-based
StacNAS (AA)	23.12	5.9	5.7	20	SGD	Cell-based

4.2 NAS Benchmarks on IMAGENET

We directly search using the whole IMAGENET dataset without subsampling on the original DARTS search space. In the first stage, 11 cells and 22 channels are used for the proxy search supernet; in the second stage, 14 cells and 22 channels are used. After the search converges, the discovered cells are stacked to form a 14 cells and 48 channel network. As shown in Table 5, we achieve a top-1 error of 23.12%, which is the best-known performance to date based on the cell-based search space. Other training details are provided in Appendix B.

4.3 Ablation Experiments

Effectiveness of operator clustering: As shown in Figure 4, although some other DARTS-alike algorithms fail to outperform the random baseline under some unbalanced search spaces, our operator clustering-based hierarchical search algorithm performs always beat the random baseline as well as the other algorithms across all search spaces. Especially, most of the DARTS-alike algorithms would discover cells dominated by *SkipConnect* or *Sep3×3* (Appendix G), while our algorithm avoided this failure and found well-mixed cells (Appendix G).

Effectiveness of complexity match via gradient confusion: in this part, we examine the effectiveness of complexity match by comparing the performance of the proposed algorithm under different width/depth combination settings on CIFAR10:

Table 6: Complexity match: different width (channels)/depth (cells) settings for search stage 1.

	Final	Match1	Match2	Match3	Poor1	Poor2	Poor3
Channels	36	32	16	10	16	16	16
Cells	20	17	14	11	5	17	20
Confusion	0.57	0.58	0.56	0.55	0.36	0.87	1.02
Error (%)	-	2.52 ± 0.09	2.48 ± 0.08	2.5 ± 0.08	2.87 ± 0.09	2.95 ± 0.12	3.12 ± 0.15
No_Skip	-	2	2	2	0	3	4

Contribution of each component: In Table 7, we conduct experiments to check how much each of the proposed components including hierarchical search via clustering, complexity matching, and one-level optimization contributes to the final performance.

Table 7: Ablation Experiments. * This result is reproduced by us using the publically available code.

	CIFAR10	
	two-level	one-level
DARTS baseline	2.97±0.32*	2.74±0.12
operator clustering	2.82±0.26	2.68±0.10
clustering+depth match	2.73±0.23	2.48±0.08

Selection of representative operators: We also experiment on CIFAR10 with randomly selected operators from each group for stage 1. The results for CIFAR10 are 2.53 ± 0.08 , which means the selection of the operators for the first stage is not sensitive.

Predicted Performance Correlation (CIFAR-10) In DARTS, the learned architecture parameter α is supposed to represent the relative importance of one candidate operator verse the others. In this part, we check the correlation between the accuracy of a stand-alone architecture with different candidate operators and the corresponding α . For the original DARTS algorithm, this correlation is as low as only 0.2, while our algorithm, achieves a surprisingly high correlation of 0.9. This results provide strong evidence what the properly learned α in the differential NAS framework is trustworthy. Detailed implementation and correlation results are provided in Appendix D.

5 Conclusion

This paper introduced a hierarchical search solution via operator clustering to differentiable NAS. Our method addresses some difficulties encountered in the original DARTS algorithm such as grouping of correlated operators, and the fundamental challenges of matching neural network optimization complexity in NAS and in the final training. It was shown that our method leads to the state-of-the-art image classification results on multiple benchmark datasets and search spaces.

References

- [1] Barret Zoph and Quoc V Le. Neural architecture search with reinforcement learning. *ICLR*, 2017.
- [2] Gabriel Bender, Pieter-Jan Kindermans, Barret Zoph, Vijay Vasudevan, and Quoc Le. Understanding and simplifying one-shot architecture search. In *ICML*, pages 549–558, 2018.
- [3] Hanxiao Liu, Karen Simonyan, and Yiming Yang. DARTS: Differentiable architecture search. In *ICLR*, 2019.
- [4] Zichao Guo, Xiangyu Zhang, Haoyuan Mu, Wen Heng, Zechun Liu, Yichen Wei, and Jian Sun. Single path one-shot neural architecture search with uniform sampling. *arXiv preprint arXiv:1904.00420*, 2019.
- [5] Sirui Xie, Hehui Zheng, Chunxiao Liu, and Liang Lin. SNAS: stochastic neural architecture search. In *International Conference on Learning Representations*, 2019.
- [6] Han Cai, Ligeng Zhu, and Song Han. ProxylessNAS: Direct neural architecture search on target task and hardware. In *ICLR*, 2019.
- [7] Zhaohui Yang, Yunhe Wang, Xinghao Chen, Boxin Shi, Chao Xu, Chunjing Xu, Qi Tian, and Chang Xu. Cars: Continuous evolution for efficient neural architecture search. *CVPR*, 2020.
- [8] Arber Zela, Thomas Elsken, Tonmoy Saikia, Yassine Marrakchi, Thomas Brox, and Frank Hutter. Understanding and robustifying differentiable architecture search. In *ICLR*, 2020.
- [9] Karthik A Sankararaman, Soham De, Zheng Xu, W Ronny Huang, and Tom Goldstein. The impact of neural network overparameterization on gradient confusion and stochastic gradient descent. *arXiv preprint arXiv:1904.06963*, 2019.
- [10] Yuhui Xu, Lingxi Xie, Xiaopeng Zhang, Xin Chen, Guo-Jun Qi, Qi Tian, and Hongkai Xiong. Pc-darts: Partial channel connections for memory-efficient architecture search. In *International Conference on Learning Representations*, 2020.
- [11] Xin Chen, Lingxi Xie, Jun Wu, and Qi Tian. Progressive differentiable architecture search: Bridging the depth gap between search and evaluation. In *ICCV*, pages 1294–1303, 2019.
- [12] Barret Zoph, Vijay Vasudevan, Jonathon Shlens, and Quoc V Le. Learning transferable architectures for scalable image recognition. In *Proceedings of the IEEE conference on computer vision and pattern recognition*, pages 8697–8710, 2018.

- [13] G Anandalingam and Terry L Friesz. Hierarchical optimization: An introduction. *Annals of Operations Research*, 34(1):1–11, 1992.
- [14] Kaiming He, Xiangyu Zhang, Shaoqing Ren, and Jian Sun. Identity mappings in deep residual networks. In *European conference on computer vision*, pages 630–645. Springer, 2016.
- [15] Bin Liu, Chenxu Zhu, Guilin Li, Weinan Zhang, Jincai Lai, Ruiming Tang, Xiuqiang He, Zhenguo Li, and Yong Yu. Autofis: Automatic feature interaction selection in factorization models for click-through rate prediction. *arXiv preprint arXiv:2003.11235*, 2020.
- [16] Dimitrios Stamoulis, Ruizhou Ding, Di Wang, Dimitrios Lymberopoulos, Bodhi Priyantha, Jie Liu, and Diana Marculescu. Single-path nas: Designing hardware-efficient convnets in less than 4 hours. *arXiv preprint arXiv:1904.02877*, 2019.
- [17] Alex Krizhevsky, Vinod Nair, and Geoffrey Hinton. Cifar-10 and cifar-100 datasets. *URL: <https://www.cs.toronto.edu/kriz/cifar.html>*, 6, 2009.
- [18] Hieu Pham, Melody Guan, Barret Zoph, Quoc Le, and Jeff Dean. Efficient neural architecture search via parameters sharing. In *ICML*, pages 4095–4104, 2018.
- [19] Esteban Real, Alok Aggarwal, Yanping Huang, and Quoc V Le. Regularized evolution for image classifier architecture search. In *Proceedings of the aaai conference on artificial intelligence*, volume 33, pages 4780–4789, 2019.
- [20] Mingxing Tan and Quoc V Le. Efficientnet: Rethinking model scaling for convolutional neural networks. *arXiv preprint arXiv:1905.11946*, 2019.
- [21] Ekin D Cubuk, Barret Zoph, Dandelion Mane, Vijay Vasudevan, and Quoc V Le. Autoaugment: Learning augmentation policies from data. *arXiv preprint arXiv:1805.09501*, 2018.
- [22] Jie Hu, Li Shen, and Gang Sun. Squeeze-and-excitation networks. In *Proceedings of the IEEE conference on computer vision and pattern recognition*, pages 7132–7141, 2018.

A Operator Correlation Estimation

We Compute the correlations among different operators using CIFAR-10. This is for the purpose of grouping similar operators in our procedure. The correlation measures are obtained as follows.

1. A network of 14 cells is trained 80 epochs using parameters in the original DARTS, where the cell DAG consists four intermediate nodes and fourteen learnable edges, and each edge is a weighted summation of all the candidate operators in the space.
2. With the trained model, for a given training image, we may pass it through the network, and store the output of the candidate operators (exclude "none" and "skip_connect") on all edges. On each edge, flatten the output tensors into vectors. Repeat until more than 10000 images in the training set have been processed.
3. Use the resulting data to calculate the correlations among the operators.

The clustering results for S1 to S5 are listed in the following table:

S1	Key Operator	Other Members
Group1	MaxPool 3×3	AvePool 3×3
Group2	SkipConnect	-
Group3	SepConv 3×3	SepConv 5×5
Group4	DilConv 3×3	DilConv 5×5

S5	Key Operator	Other Members
Group1	SkipConnect	-
Group2	SepConv 3×3	-

S3	Key Operator	Other Group Members
Group1	MaxPool 3×3	-
Group2	SkipConnect	-
Group3	SepConv 3×3	SepConv 5×5 , SepConv 7×7
Group4	DilConv 3×3	DilConv 5×5

B Train Details

CIFAR-10 and CIFAR-100 The final architecture is a stack of 20 cells: 18 normal cells and 2 reduction cells, positioned at the 1/3 and 2/3 of the network respectively.

ImageNet The final architecture is a stack of 14 cells: 12 normal cells and 2 reduction cells, positioned at the 1/3 and 2/3 of the network respectively. For the *base* training, we trained the network exactly the same with DARTS. For the AA training, we add AutoAugment (IMAGENET) [21] policy and SE [22], then trained the network for 600 epochs, other than these, all the other settings are same as DARTS.

C Estimation of Gradient Confusion

We compared gradient confusion for several different settings, including different numbers of cells, different stages, with/without an auxiliary head. The result are provided in the following table.

For each setting, we first train the architecture for 100 epochs and then ran 10 more iterations with randomly selected mini-batch using the trained parameters and compute the gradient confusion using formula (3.4.2) and obtain ζ_i for each iteration i . Then, we compute the mean of the 10 ζ_i we got and divided them by the corresponding model parameter size M . Formally,

$$\bar{\zeta} = \sum_{i=1}^{10} \zeta_i / M \quad (2)$$

We treat it as the measurement of the optimization complexity for the corresponding setting.

S4	Key Operator	Other Group Members
Group1	SkipConnect	-
Group2	SepConv 3×3	SepConv 5×5 , DilConv 3×3 , DilConv 5×5

S2	Key Operator	Other Group Members
Group1	SkipConnect	MaxPool 3×3 , MaxPool 5×5 , AvePool 3×3 , AvePool 5×5
Group2	SepConv 3×3	SepConv 5×5

D Predicted Performance Correlation

In DARTS, the learned architecture parameter α is supposed to represent the relative importance of one candidate operator verse the others. To check the correlation between the accuracy of a stand-alone architecture with different candidate operators and the corresponding α , we replace the selected operator in the first edge of the first cell for the final architecture with all the other candidate operators, and fully train them until converge. The obtained stand-alone accuracy is compared with the corresponding α learned for each candidate operator. Their correlation is plotted in Figure 5.

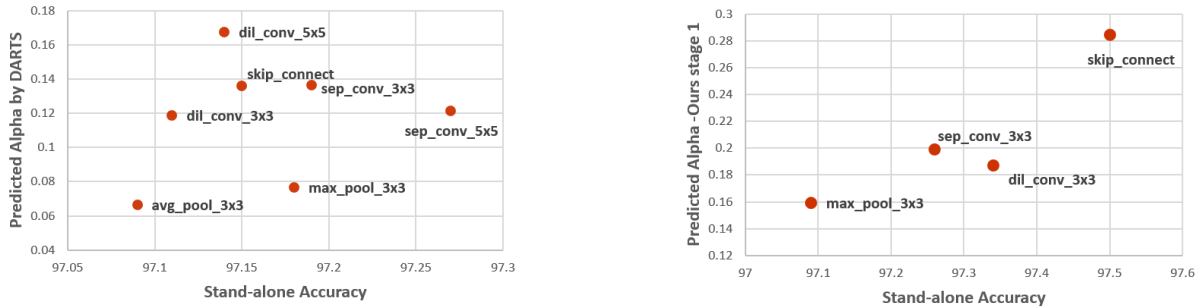


Figure 5: Correlation between standalone model and learned α : (a) Correlation coefficient of StacNAS: 0.91; (b) Correlation coefficient of DARTS: 0.2.

E The Algorithm

F CIFAR10 Benchmark Table

G Cells of Benchmark Dataset

Algorithm 1 Hierarchical NAS via operator Clustering

- 1: **procedure** STAGE 1 (Group search)
 - 2: Create a by-group operator $\tilde{o}^{(i,j)}(x)$ parametrized by $\tilde{\alpha}_o^{(i,j)}$ for each edge (i, j)
 - 3: **if** $t < T$ **then**
 - 4: Update weights w_t by descending $\partial_w L_{train}(w_{t-1}, \tilde{\alpha}_{t-1})$
 - 5: Update architecture parameter $\tilde{\alpha}_t$ by descending $\partial_{\tilde{\alpha}} L_{train}(w_{t-1}, \tilde{\alpha}_{t-1})$
 - 6: Set optimal $\tilde{\alpha}^* = \alpha^T$
 - 7: Activate the optimal operator group based on $\tilde{\alpha}^*$
 - 8: **procedure** STAGE 2 (Backward)
 - 9: Use all the group member of $o^{*(i,j)}$ to create mixed operator $\hat{o}^{(i,j)}(x)$ parametrized by $\hat{\alpha}_o^{(i,j)}$
 - 10: **if** $t < T$ **then**
 - 11: Update weights w_t by descending $\partial_w L_{train}(w_{t-1}, \hat{\alpha}_{t-1})$
 - 12: Update architecture parameter $\hat{\alpha}_t$ by descending $\partial_{\hat{\alpha}} L_{train}(w_{t-1}, \hat{\alpha}_{t-1})$
 - 13: Set optimal $\hat{\alpha}^* = \alpha^T$
 - 14: Select the best operator $o^{*(i,j)} \leftarrow \operatorname{argmax}_{o \in O} \hat{\alpha}^{(i,j)}$
 - 15: **procedure** STAGE 3 (Final Architecture)
 - 16: Prune the redundant operators and edges.
-

	Random	DARTS	CARS	PC_DARTS	Robust_DARTS	StacNAS
S2	96.59 ± 0.60	96.78 ± 0.20	97.06 ± 0.10	97.28 ± 0.09	96.81 ± 0.15	97.46 ± 0.08
S3	97.14 ± 0.16	91.87 ± 3.30	96.95 ± 0.22	97.09 ± 0.15	97.23 ± 0.09	97.57 ± 0.09
S4	96.81 ± 0.15	88.36 ± 5.10	97.19 ± 0.09	97.16 ± 0.15	97.14 ± 0.19	97.35 ± 0.11
S5	97.31 ± 0.15	95.67 ± 1.20	97.19 ± 0.22	97.05 ± 0.13	97.23 ± 0.11	97.40 ± 0.08

Table 8: Results of different search algorithms on various search space base on CIFAR10. Means and stds are obtained by repeated experiments with 4 seeds.

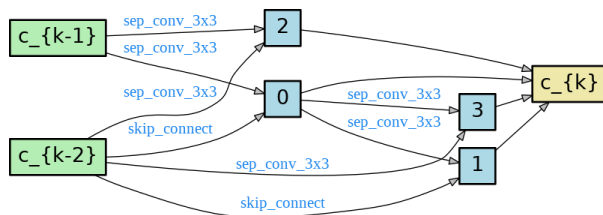


Figure 6: Normal cell learned on CIFAR-10 for S1 (StacNAS)

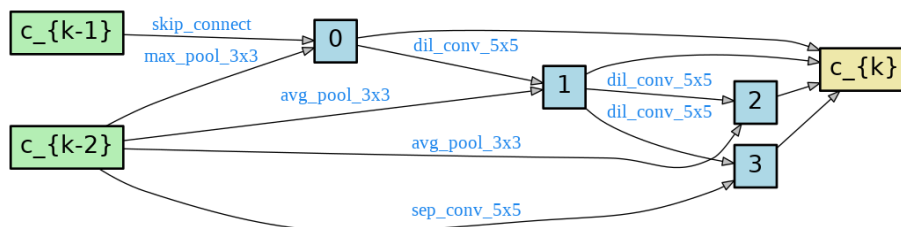


Figure 7: Reduction cell of CIFAR-10 for S1 (StacNAS)

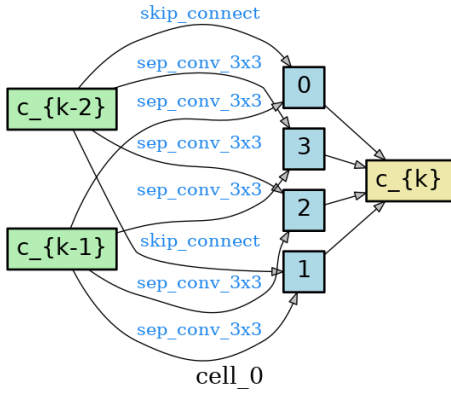


Figure 8: Normal cell of CIFAR-10 for S2 (StacNAS)

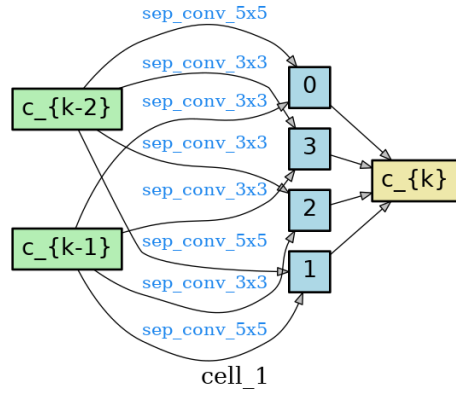


Figure 9: Reduction cell of CIFAR-10 for S2 (StacNAS)

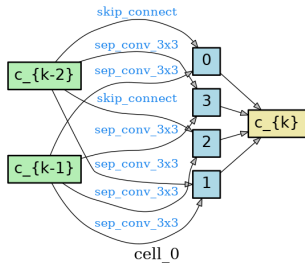


Figure 10: Normal cell of CIFAR-10 for S3 (StacNAS)

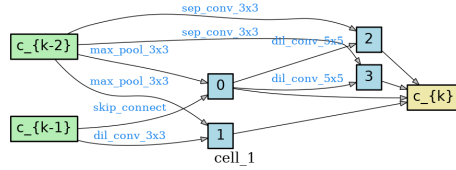


Figure 11: Reduction cell of CIFAR-10 for S3 (StacNAS)

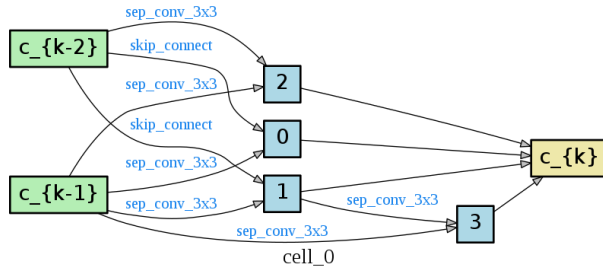


Figure 12: Normal cell of CIFAR-10 for S4 (StacNAS)

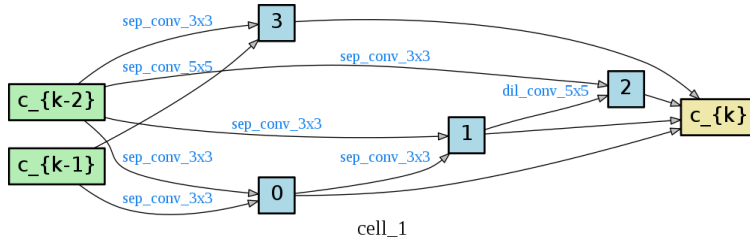


Figure 13: Reduction cell of CIFAR-10 for S4 (StacNAS)

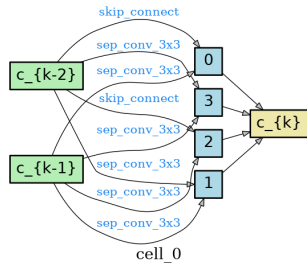


Figure 14: Normal cell of CIFAR-10 for S5 (StacNAS)

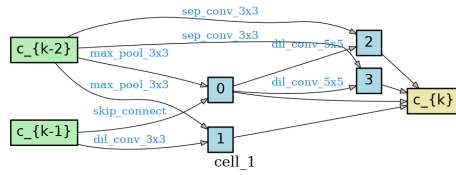


Figure 15: Reduction cell of CIFAR-10 for S5 (StacNAS)

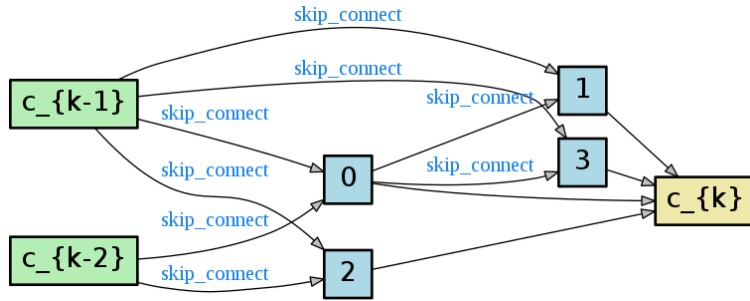


Figure 16: A cell dominated by SkipConnect discovered by DARTS

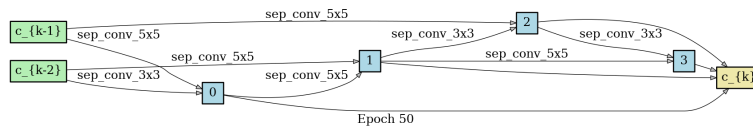


Figure 17: A cell dominated by SepConv discovered by DARTS